Electronic Supporting Information

Structural characterization of a highly active superoxide-dismutase mimic

Vimalkumar Balasubramanian,[a#] Maria Ezhevskaya,[b,#] Hans Moons,[b] Markus Neuburger,[a] Carol Cristescu,[c] Sabine Van Doorslaer[b*] and Cornelia Palivan[a*]

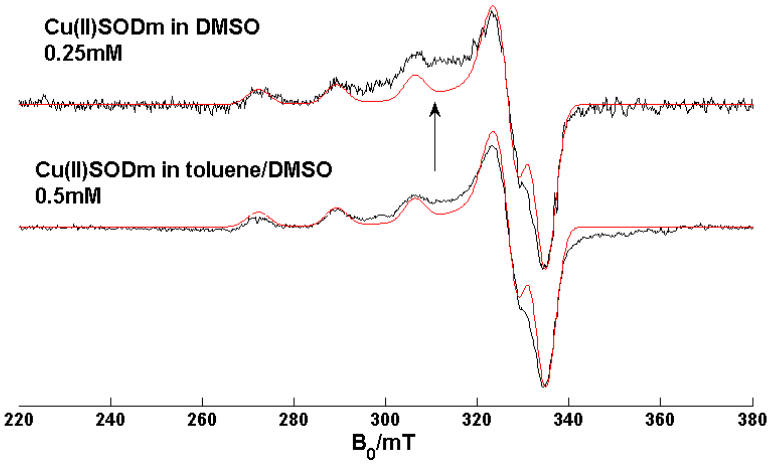

Figure S1. X-band CW-EPR spectra of the Cu^{II}SODm in frozen DMSO and in frozen DMSO:toluene (1:1). It was found that DMSO formed a bad glass leading to local clustering of the copper complexes as is exemplified by the top spectrum. The broad signal underneath the type-2 Cu^{II} EPR spectrum is due to clustered copper complexes. The relative contribution of this broad signal increased upon increase of the concentration of the Cu^{II}SODm. Addition of toluene largely solved this problem. However, a small fraction of clustered CuII complexes is still present. The ESE-detected EPR spectrum (see for instance Figure S3) showed that this fraction does not contribute to the electron spin echo as is expected due to the fast phase-memory times expected for clustered complexes (due to the dipolar interactions). Note that the complex was not soluble in pure toluene.

Table S1. UV/Vis absorption and IR-spectroscopic data for the free ligand **L** and the related Cu^{II}SODm. The UV/Vis data relate to the solutions in DMSO (similar values for DMSO:toluene), IR data relate to the powders.

Compound	λ_{max} (nm)			IR (cm^{-1})				
	ILT	LMCT	d-d	*ν*(OH)	*ν*(CH=N)	*ν*(C=N)	*ν*(NH)	*ν*(C=O)
L	303	-	-	~3250-3280	~1648	~1565	~3150	~1680
Copper complex	353, 380(sh),	428, 482(sh)	678	-	~1630	~1584	~3150	~1682

Table S2. Selected bond distances (Å) and the angles (º) for the Cu^{II}SODm under study.

Bond lengths/ Å		Bond angles/ °	
Cu_1-N_1	1.964(3)	N_1-Cu_1-N_5	79.57(12)
Cu_1-N_5	2.000(3)	Cl_1^i-Cu_1-N_5	89.48(9)
Cu_1-O_1	1.900(2)	Cl_1^i-Cu_1-N_1	113.64(9)
Cu_1-Cl_1	2.308(1)	Cl_1-Cu_1- N_5	95.03(9)
Cu_1-Cl_1^i	2.645(1)	O_1-Cu_1-N_1	91.90(11)
Cu_1-Cu_1^i	3.468(1)	O_1-Cu_1-N_5	170.66(12)
		Cl_1^i-Cu_1-O_1	90.49(8)
		Cl_1^i-Cu_1-Cl_1	91.40(3)
		Cl_1-Cu_1-O_1	94.31(8)
		Cl_1-Cu_1-N_1	154.16(9)
		Cl_1^i -Cl_1-Cu_2	88.60(3)

Foot note: (i = 1-x, 1-y, 1-z)

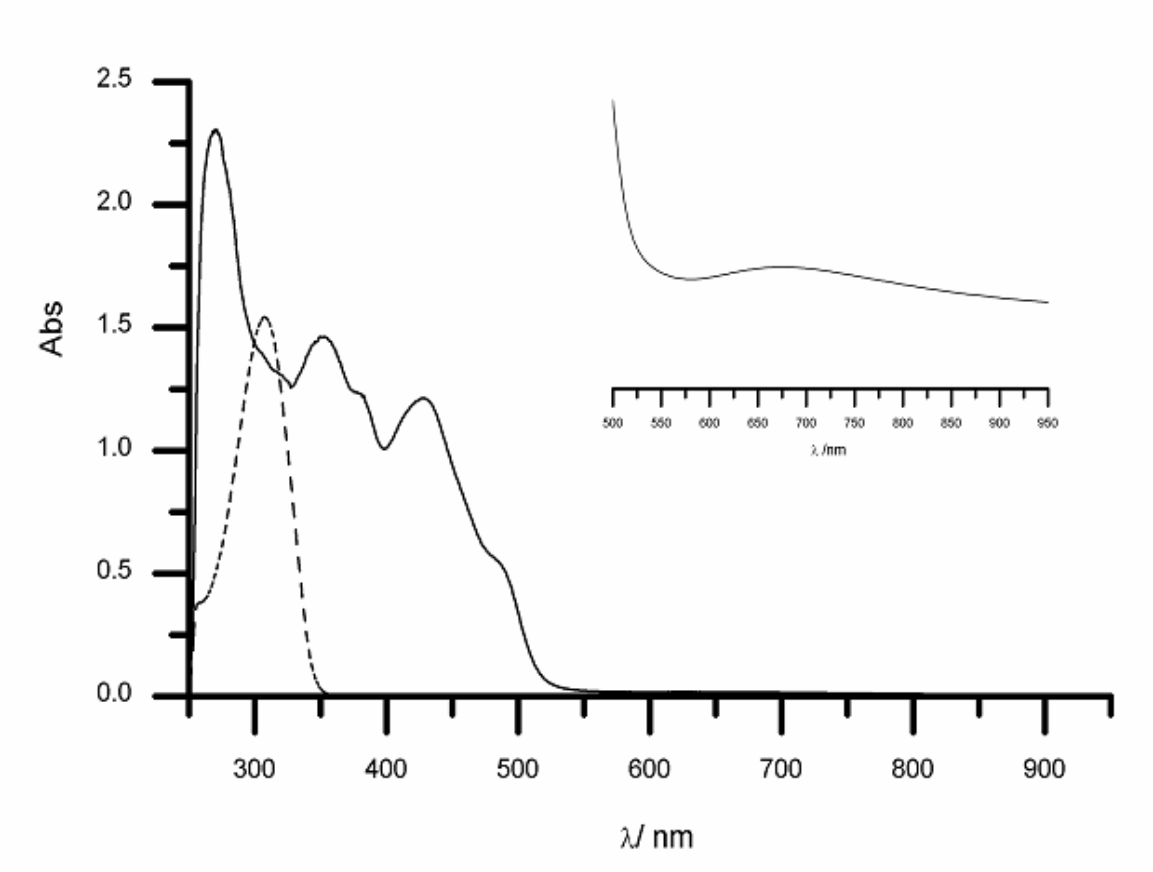

Figure S2. UV/Vis absorption spectrum of a DMSO solution of the Cu^{II}SODm under study. Free ligand = dashed line, complex = full line

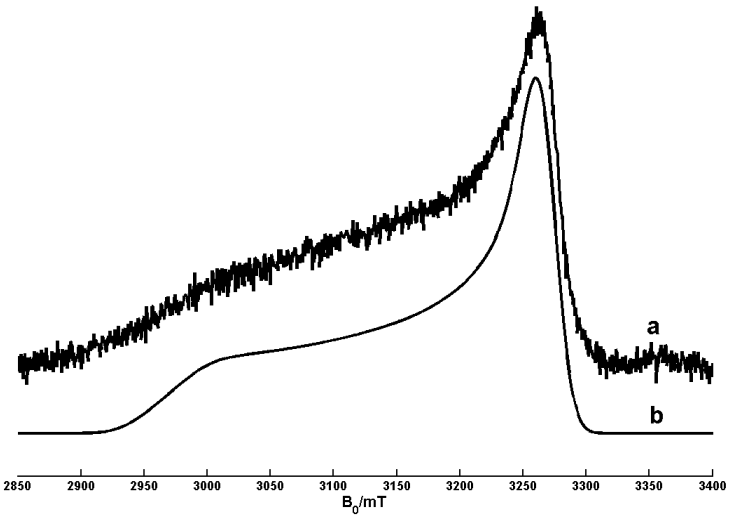

Figure S3. W-band ESE-detected EPR spectrum of a frozen DMSO:toluene solution of the Cu^{II}SODm under study. (a) Experimental spectrum. (b) Simulation using the data in Table 2 (main text). The spectrum proves that there is no significant ***g*** rhombicity.

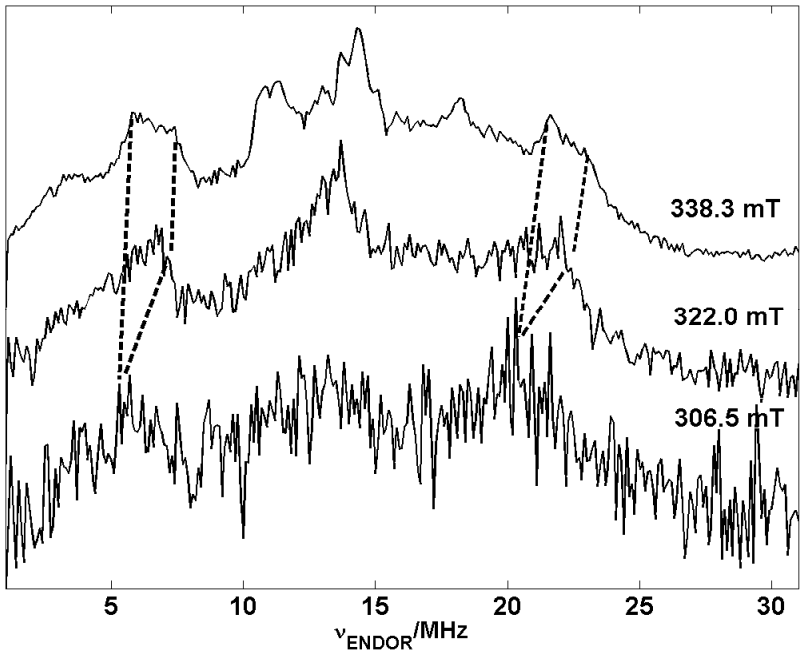

Figure S4. X-band Davies-ENDOR spectra of a frozen DMSO:toluene solution of the Cu^{II}SODm under study taken at different magnetic-field settings. Due to the small echo intensity, the Davies-ENDOR spectra taken at low magnetic field settings are of poor quality.

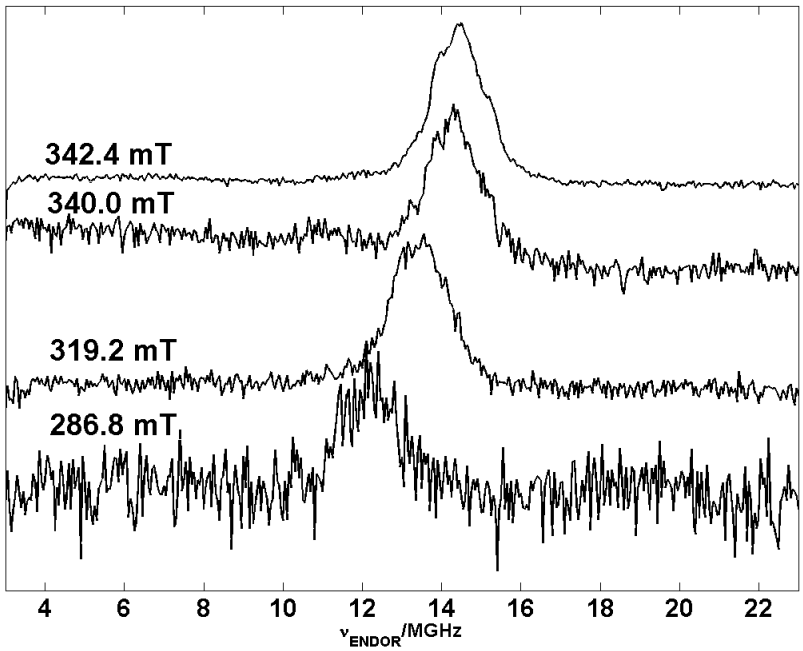

Figure S5. X-band Mims-ENDOR spectra of a frozen DMSO:toluene solution of the Cu^{II}SODm for different settings of the magnetic field (observer positions are given in the figure). All spectra are the sum of 30 τ values.

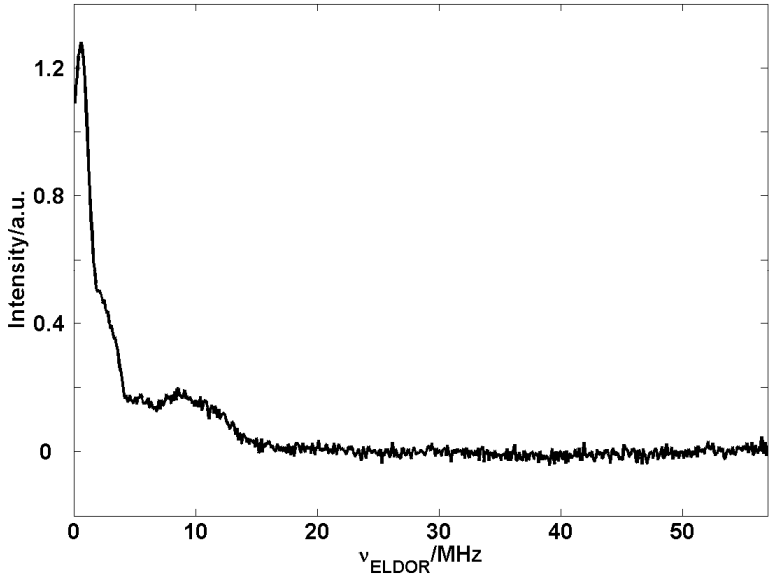

Figure S6. W-band ELDOR-detected NMR spectrum of a frozen DMSO:toluene solution of the Cu^{II}SODm taken at an observer position corresponding with $g \approx g_{\perp}$. The signal around 10 MHz is most probably due to the interaction with N_1 and/or N_5 (nuclear frequencies of the m_S=1/2 manifold). However, since the corresponding nuclear frequency of the m_S=-1/2 manifold is not observed, no definite attribution of the signal can be made.

HYSCORE simulations using parameters in Table 4 (main text)

(a)

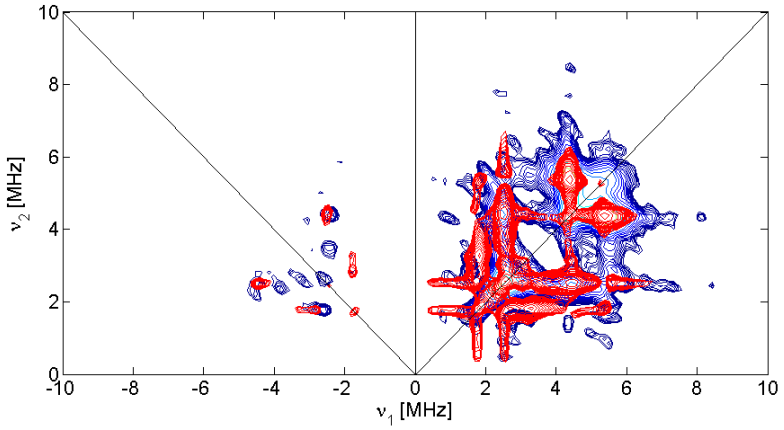

(b)

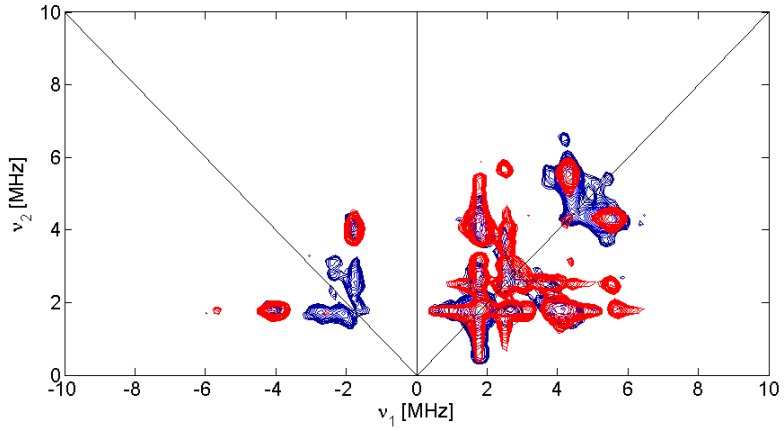

(c)

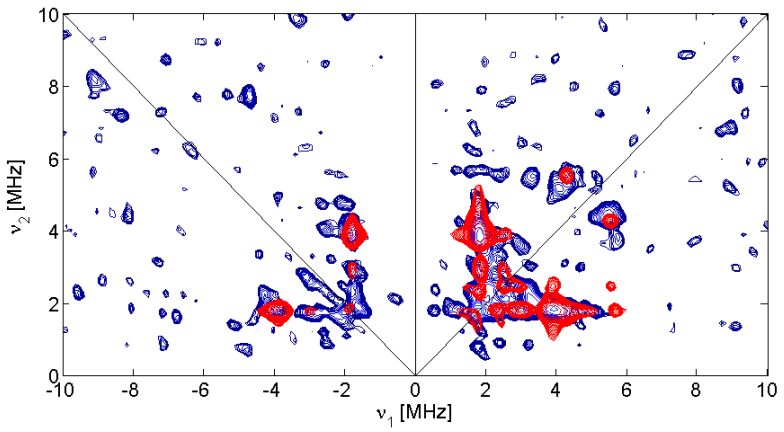

(d)

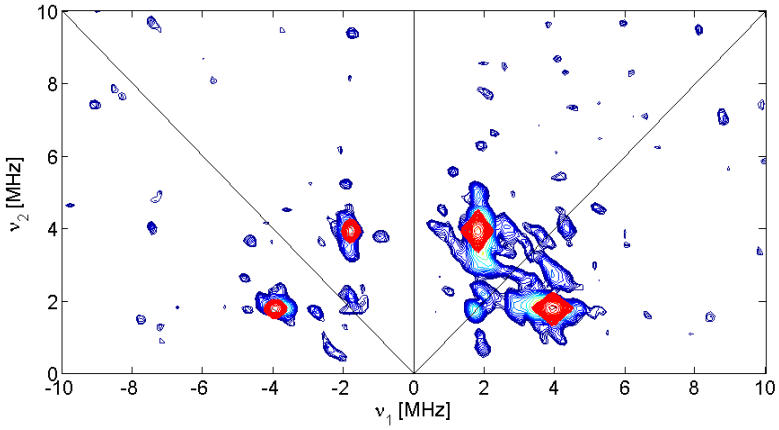

Figure S7. Experimental X-band HYSCORE spectra (blue) taken at observer positions (a) B_0=343.4 mT, (b) B_0=319.6 mT, (c) B_0=303.6 mT and (d) B_0=285.2 mT overlain with the simulation (red) assuming a two-spin (S=1/2, I=1) system and using the parameters given in Table 4 of the main text.

HYSCORE simulations assuming two sets on nitrogen nuclei

(a) (b)

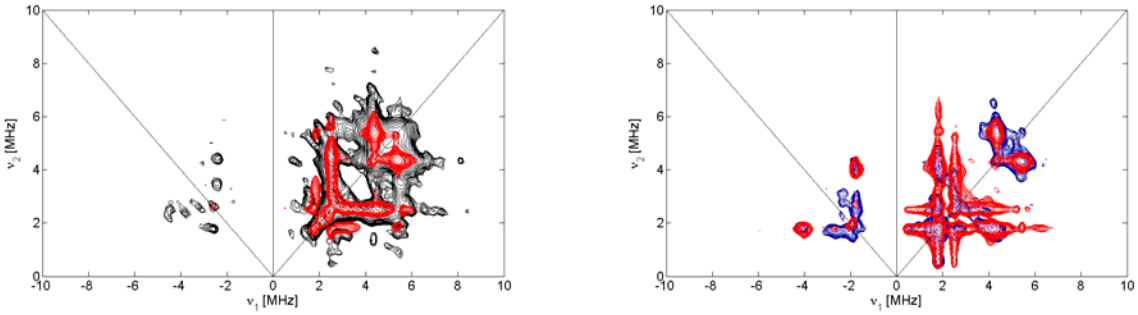

(c) (d)

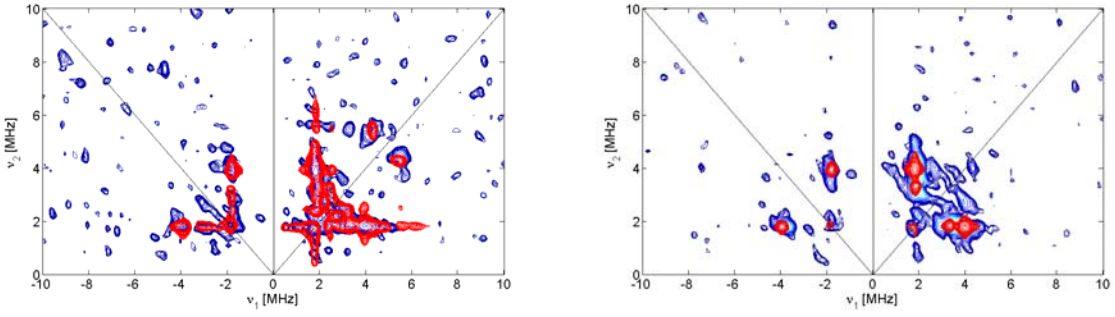

Figure S8. Experimental X-band HYSCORE spectra (blue) taken at observer positions (a) B_0=343.4 mT, (b) B_0=319.6 mT, (c) B_0=303.6 mT and (d) B_0=285.2 mT overlain with the simulation (red) assuming a three-spin system (S=1/2, I_1=1, I_2=1) with $\boldsymbol{A_1}$=[1 1.9 1.25 MHz], $(e^2Qq/h)_1$=-4.5 MHz and η_1=0.8 and $\boldsymbol{A_2}$=[-1 -1.7 -1.9 MHz], $(e^2Qq/h)_2$=-4.5 MHz and η_2=0.8,

with the hyperfine and nuclear quadrupole tensor of the second nucleus rotated 20° about the z axis. This simulates the contribution of a N_2-like and a N_4-like nitrogen (see Tables S10 and S12) and proves that the experimental data are consistent with the DFT data.

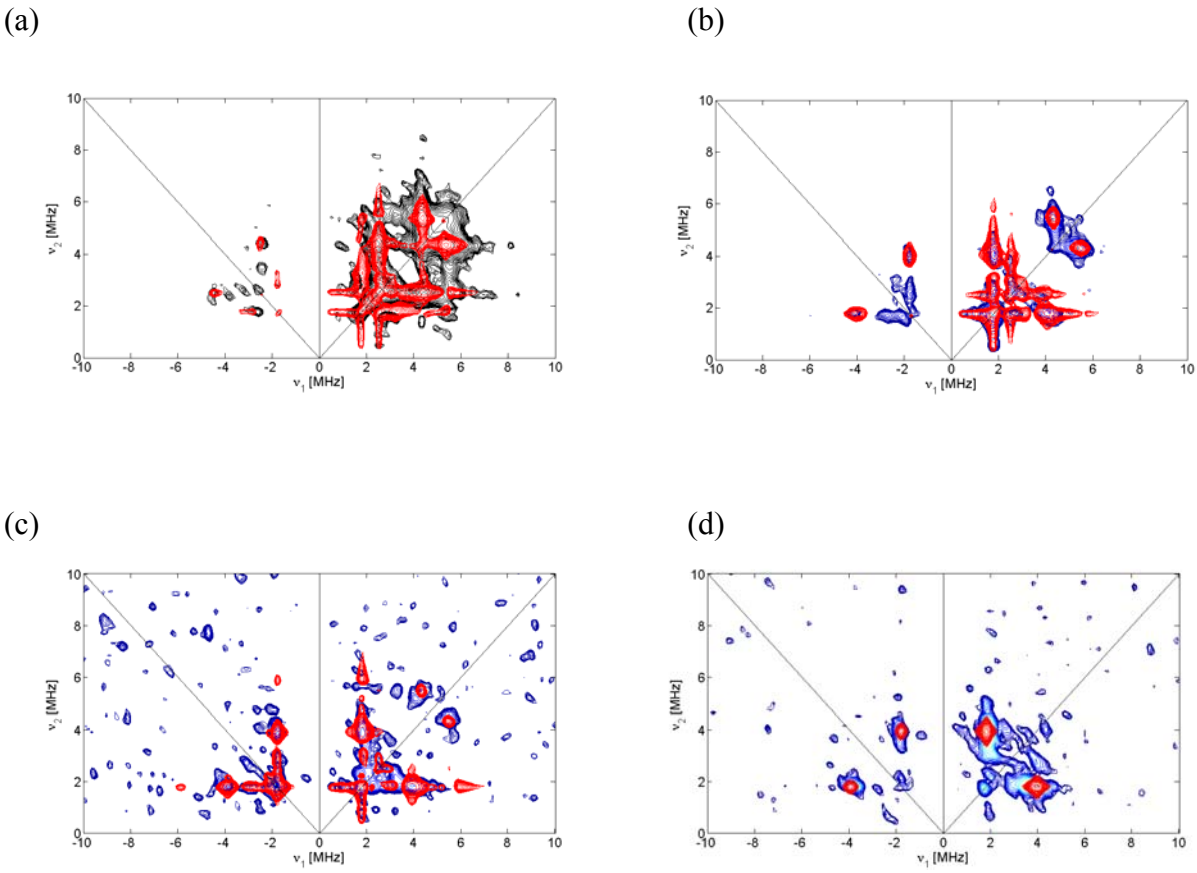

Figure S9. Experimental X-band HYSCORE spectra (blue) taken at observer positions (a) B_0=343.4 mT, (b) B_0=319.6 mT, (c) B_0=303.6 mT and (d) B_0=285.2 mT overlain with the simulation (red) assuming a three-spin system (S=1/2, I_1=1, I_2=1) with $\boldsymbol{A_1}$=[-1 -1.7 -1.9 MHz], $(e^2Qq/h)_1$=-4.5 MHz and η_1=0.8 and $\boldsymbol{A_2}$=[-0.03 -0.09 0.16 MHz], $(e^2Qq/h)_2$=-3.4 MHz and η_2=0.265. α_2=90° for the $\mathbf{P}_2$ tensor, all other Euler angles of the hyperfine and nuclear quadrupole tensors are 0°. This simulates the contribution of a N_2 and a N_3-like nitrogen. The shallow modulation of the N_3 nucleus hardly alters the HYSCORE patterns (compare with Figure S7).

S10. Optimized structures of models used in DFT computations

MODEL A, [Cu**L**Cl] - Optimized structure

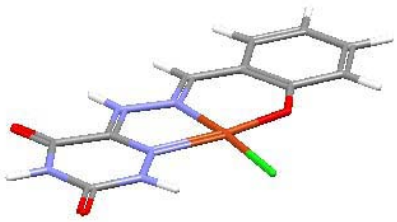

Coordinates from ORCA output

O	-7.191423	-1.467730	-0.138589
O	-5.302800	2.729023	-0.021500
O	0.023205	-1.431306	-0.108580
C	3.246251	1.209012	-0.020662
C	3.418664	-0.193326	-0.050976
C	2.329901	-1.047588	-0.080408
C	0.994579	-0.554159	-0.081011
C	0.822806	0.874931	-0.049955
C	1.964941	1.722715	-0.020327
C	-0.457675	1.506519	-0.045475
N	-1.589610	0.859054	-0.072101
N	-2.769410	1.553809	-0.062198
C	-3.896090	0.812961	-0.077998
N	-3.784033	-0.488353	-0.111865
Cu	-1.852592	-1.120090	-0.124858
Cl	-2.430931	-3.334153	-0.202689
N	-4.916648	-1.249314	-0.135029
C	-6.195717	-0.764207	-0.119634
N	-6.263918	0.638516	-0.080084
C	-5.205154	1.514411	-0.056536
H	-0.488152	2.598933	-0.017349
H	-2.800560	2.567071	-0.010779
H	-4.742894	-2.249193	-0.161399
H	-7.199443	1.033105	-0.067109

H	4.108295	1.870786	0.002060
H	4.423775	-0.612374	-0.051313
H	2.461901	-2.126918	-0.103558
H	1.805730	2.799865	0.002918

MODEL B, [Cu**L**(DMSO)]$^{+}$ - Optimized structure

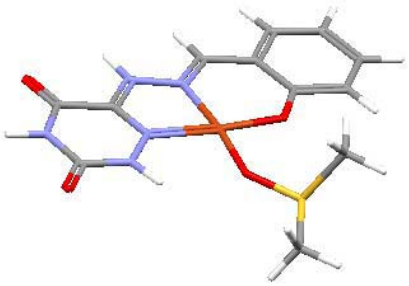

Coordinates from ORCA output

O	-7.420211	-0.717816	-0.098897
O	-5.195902	3.305477	-0.358725
O	-0.280953	-1.316471	0.045866
C	3.199309	0.971623	-0.137026
C	3.227819	-0.435332	-0.023325
C	2.056006	-1.171939	0.033931
C	0.782298	-0.546264	-0.018853
C	0.753269	0.888444	-0.136386
C	1.976958	1.611772	-0.191614
C	-0.452729	1.655306	-0.204143
N	-1.647314	1.133997	-0.172964
N	-2.760100	1.928350	-0.244659
C	-3.948103	1.287489	-0.206869
N	-3.947285	-0.015799	-0.113039
Cu	-2.092946	-0.781667	-0.036081
O	-2.820156	-2.591004	0.119370
N	-5.134913	-0.686327	-0.082363
C	-6.371602	-0.098698	-0.132800
N	-6.322123	1.301731	-0.230435
C	-5.196037	2.090162	-0.274540
H	-0.363458	2.741282	-0.288521
H	-2.701465	2.940517	-0.294791

H	-5.048524	-1.692720	-0.004874
H	-7.222361	1.770108	-0.270803
H	4.124224	1.540799	-0.181276
H	4.184343	-0.953614	0.020195
H	2.077960	-2.255765	0.120710
H	1.929872	2.696060	-0.280041
S	-1.905618	-3.856769	-0.127186
C	-1.210602	-4.249490	1.499110
C	-3.131797	-5.179773	-0.268971
H	-2.017130	-4.305276	2.237115
H	-0.510022	-3.444461	1.737149
H	-0.679462	-5.204073	1.417602
H	-3.797342	-5.150026	0.599267
H	-2.591750	-6.130924	-0.323663
H	-3.685149	-5.007907	-1.196471

MODEL C, [Cu**L**$(DMSO)_2]^+$ - Optimized structure

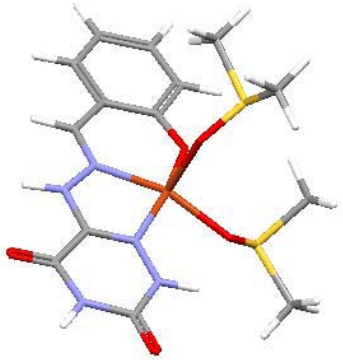

Coordinates from ORCA-output

O	-2.277671	-0.967250	-2.994366
S	-1.254807	-0.955718	-4.188673
C	-2.327628	-1.134839	-5.637235
C	-0.489753	-2.599409	-4.178194
H	-2.905692	-0.210768	-5.728117
H	-2.986210	-1.997253	-5.493289
H	-1.688862	-1.266391	-6.517069
H	0.113498	-2.645526	-3.267722
H	0.147425	-2.683545	-5.065313
H	-1.270161	-3.367067	-4.175089

O	-6.806830	1.016864	-2.301925
O	-4.775361	3.181441	1.217299
O	0.132893	-0.684122	-1.423098
C	3.453595	0.378176	0.867805
C	3.541930	-0.524165	-0.212993
C	2.421594	-0.858776	-0.956585
C	1.139046	-0.315765	-0.666893
C	1.052542	0.606620	0.437605
C	2.223407	0.928480	1.175490
C	-0.160250	1.261006	0.840646
N	-1.315057	1.058522	0.280139
N	-2.423715	1.742452	0.709263
C	-3.543042	1.580101	-0.039583
N	-3.514416	0.729728	-1.026369
Cu	-1.715926	-0.214496	-1.213984
O	-2.364670	-1.962722	-0.012354
N	-4.636788	0.528327	-1.770165
C	-5.824723	1.190129	-1.600967
N	-5.809167	2.094823	-0.527938
C	-4.748785	2.374606	0.303944
H	-0.098695	1.977789	1.664366
H	-2.347641	2.520730	1.357402
H	-4.514206	-0.110458	-2.546765
H	-6.674736	2.600923	-0.367462
H	4.336514	0.637177	1.446680
H	4.503220	-0.966519	-0.470375
H	2.491898	-1.552024	-1.791947
H	2.131504	1.630369	2.003343
S	-1.783207	-3.357000	-0.348555
C	-0.558429	-3.721635	0.947379
C	-3.061264	-4.542784	0.166995
H	-1.013538	-3.577991	1.933358
H	0.276261	-3.028257	0.805142
H	-0.211412	-4.752902	0.820046
H	-3.345337	-4.343553	1.205868
H	-2.661351	-5.556495	0.055632
H	-3.917998	-4.403831	-0.499376

MODEL D, [Cu**L**$(DMSO)_3]^+$ - Optimized structure

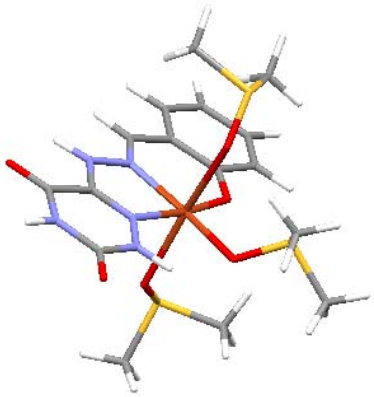

Coordinates from ORCA-output

O	-2.076924	-0.208903	-2.708571
S	-0.959340	-0.074905	-3.763038
C	-1.766372	0.588076	-5.254942
C	-0.616595	-1.750091	-4.391899
H	-2.092962	1.606457	-5.022718
H	-2.625529	-0.040155	-5.514400
H	-1.033957	0.607567	-6.069463
H	-0.165589	-2.297841	-3.559777
H	0.086946	-1.673811	-5.228253
H	-1.554064	-2.221134	-4.707069
O	-6.896226	-1.262272	-0.002125
O	-4.539642	2.348692	1.615182
O	0.247805	-1.647132	-1.104015
C	3.728392	0.556261	-0.453424
C	3.740040	-0.699709	-1.098453
C	2.568534	-1.410503	-1.295663
C	1.303491	-0.914907	-0.865939
C	1.297536	0.366285	-0.200436
C	2.520833	1.066782	-0.016228
C	0.111176	1.001694	0.303615
N	-1.077739	0.483150	0.226889
N	-2.157614	1.148916	0.742811
C	-3.368663	0.564931	0.558712
N	-3.419254	-0.588038	-0.042269
Cu	-1.584391	-1.259054	-0.648482
O	-2.406472	-2.963269	-1.352858
N	-4.618272	-1.206372	-0.207224
C	-5.830084	-0.698117	0.178741

N	-5.728983	0.547712	0.817390
C	-4.577277	1.263894	1.058915
H	0.226611	1.977394	0.785015
H	-2.083145	2.093460	1.106974
H	-4.562419	-2.084191	-0.709985
H	-6.605943	0.957045	1.124505
H	4.651618	1.110039	-0.301817
H	4.683112	-1.118375	-1.447543
H	2.575629	-2.378516	-1.792101
H	2.487559	2.033021	0.486135
S	-1.802487	-4.343882	-0.918987
C	-1.981663	-5.355581	-2.415035
C	-3.096346	-5.112022	0.094667
H	-1.719901	-6.388975	-2.163126
H	-1.280155	-4.964855	-3.157950
H	-3.011185	-5.287430	-2.781058
H	-3.173437	-4.493826	0.992600
H	-2.776051	-6.127591	0.351840
H	-4.037879	-5.128564	-0.464598
O	-1.650751	-2.572339	1.504444
S	-0.808615	-2.882352	2.754916
C	0.945631	-2.647794	2.318984
C	-0.976461	-1.448583	3.868232
H	1.547913	-2.840299	3.213688
H	1.111510	-1.632256	1.945817
H	1.183451	-3.379495	1.541280
H	-0.731145	-0.531204	3.322461
H	-0.305438	-1.587514	4.722937
H	-2.015812	-1.424518	4.209697

MODEL E, [Cu**L**Cl(DMSO)] - Optimized structure

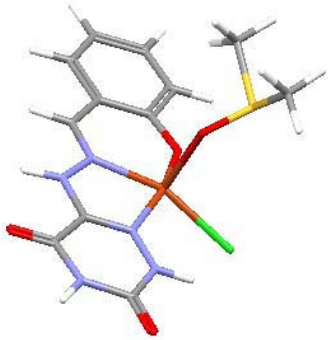

Coordinates from ORCA-output

Cl	-2.322121	-1.009490	-3.407042
O	-6.865680	0.957220	-2.226271
O	-4.758178	3.202999	1.194457
O	0.141173	-0.714835	-1.400671
C	3.429370	0.333677	0.940476
C	3.518401	-0.607041	-0.108293
C	2.407542	-0.937772	-0.866502
C	1.130489	-0.351467	-0.627075
C	1.044717	0.604749	0.448107
C	2.206398	0.922292	1.202320
C	-0.166128	1.282163	0.810028
N	-1.310517	1.086184	0.225988
N	-2.413901	1.780362	0.647827
C	-3.548444	1.586568	-0.065698
N	-3.536588	0.714927	-1.034337
Cu	-1.719094	-0.226368	-1.272990
O	-2.310860	-1.947156	0.008733
N	-4.681002	0.489246	-1.738044
C	-5.866091	1.147745	-1.553191
N	-5.832512	2.071733	-0.496402
C	-4.750912	2.377379	0.296629
H	-0.115037	2.007200	1.627772
H	-2.341771	2.550895	1.305209
H	-4.557923	-0.143350	-2.523410
H	-6.697498	2.574115	-0.322840
H	4.305613	0.589835	1.530810
H	4.473798	-1.081652	-0.328168
H	2.476910	-1.658943	-1.678237
H	2.112623	1.651259	2.006497

S	-1.709473	-3.333634	-0.320506
C	-0.465596	-3.666358	0.966961
C	-2.961609	-4.535217	0.224840
H	-0.911674	-3.515385	1.956053
H	0.358670	-2.964767	0.806214
H	-0.107366	-4.694982	0.849577
H	-3.238343	-4.326802	1.263962
H	-2.546488	-5.543823	0.122847
H	-3.827894	-4.419503	-0.433629

Computed spin Hamiltonian values

In the following Tables, the main computed spin Hamiltonian values are given for the different models. The numbering of the nuclei is given in Scheme 1.

Table S3. Computed ***g*** tensors for the different models for Cu^{II}SODm in a DMSO:toluene solution (basis sets TZVPP/6-31G)

	g_x	g_y	g_z
Model A	2.039	2.055	2.153
Model B	2.044	2.047	2.150
Model C	2.050	2.073	2.182
Model D	2.056	2.072	2.192
Model E	2.040	2.089	2.185

For the computation of the hyperfine values, the ORCA basis set 'CoreProp' (CP(III)) was used for copper, the Barone basis set 'EPR-II' for the calculated hydrogen and nitrogen atoms, and a TZVPP basis for the chlorine atom.

Table S4. Computed copper ***A*** tensors for the different models for Cu^{II}SODm in a DMSO:toluene solution

	A_x/MHz	A_y/MHz	A_z/MHz
Model A	14.87	-40.10	-578.27
Model B	-3.00	-18.21	-607.48
Model C	21.87	104.60	-540.11
Model D	44.90	99.28	-536.24
Model E	-10.52	133.88	-504.98

Table S5. Computed proton ***A*** tensors for H^a in the different models for Cu^{II}SODm in a DMSO:toluene solution. ($\mathbf{A_z}$ is perpendicular to the **L** plane, $\mathbf{A_x}$ points in the direction of the copper ion).

	A_x/MHz	A_y/MHz	A_z/MHz
Model A	22.67	19.26	18.38
Model B	23.29	19.75	18.87
Model C	21.52	18.06	17.19
Model D	20.45	16.97	16.15
Model E	20.48	17.13	16.30

Table S6. Computed proton ***A*** tensors for H^b in the different models for Cu^{II}SODm in a DMSO:toluene solution. ($\mathbf{A_x}$ is approximately along the H-N bond, $\mathbf{A_z}$ is approximately perpendicular to the plane of **L**).

	A_x/MHz	A_y/MHz	A_z/MHz
Model A	11.14	6.83	5.75
Model B	11.50	7.00	5.94
Model C	9.77	5.24	4.28
Model D	10.14	5.68	4.72
Model E	9.45	5.14	4.17

Table S7. Computed proton ***A*** tensors for H^c in the different models for Cu^{II}SODm in a DMSO:toluene solution. ($\mathbf{A_x}$ is pointing towards the copper ion, $\mathbf{A_z}$ is perpendicular to the plane of **L**).

	A_x/MHz	A_y/MHz	A_z/MHz
Model A	7.14	-0.53	1.22
Model B	7.31	1.14	-0.64
Model C	7.27	0.80	-0.611
Model D	7.32	0.82	-0.75
Model E	7.18	-0.51	0.90

Table S8. Computed proton ***A*** tensors for H^d in the different models for Cu^{II}SODm in a DMSO:toluene solution. ($\mathbf{A_z}$ is perpendicular to the plane of **L**, $\mathbf{A_y}$ is pointing in the direction of the copper ion)

	A_x/MHz	A_y/MHz	A_z/MHz
Model A	-1.85	1.73	-2.65
Model B	-1.88	1.82	-2.61
Model C	0.65	-0.65	-2.53
Model D	-1.72	1.81	-2.39
Model E	-1.79	1.76	-2.55

Table S9. Computed nitrogen hyperfine and nuclear quadrupole tensors for N_1 in the different models for Cu^{II}SODm in a DMSO:toluene solution. ($\mathbf{A_z}$ is perpendicular to the plane of **L**, $\mathbf{A_y}$ is pointing in the direction of the copper ion. The largest nuclear quadrupole coupling is approximately along $\mathbf{A_x}$, the smallest nuclear quadrupole value (in absolute value) is lying approximately perpendicular to the **L** plane)

	A_x/MHz	A_y/MHz	A_z/MHz	e^2qQ/h /MHz	η
Model A	44.02	57.37	45.89	3.761	0.434
Model B	44.91	58.84	46.88	3.759	0.426
Model C	40.99	53.74	42.90	3.785	0.549
Model D	40.92	53.23	40.92	3.810	0.618
Model E	39.13	51.11	40.90	3.788	0.580

Table S10. Computed nitrogen hyperfine and nuclear quadrupole tensors for N_2 in the different models for Cu^{II}SODm in a DMSO:toluene solution. ($\mathbf{A_z}$ and $\mathbf{P_z}$ are quasi perpendicular to the plane of **L**,

	A_x/MHz	A_y/MHz	A_z/MHz	e^2qQ/h /MHz	η
Model A	-0.05	-1.05	-1.92	-5.01	0.52
Model B	-0.07	-1.09	-1.92	-5.04	0.53
Model C	-0.25	-1.23	-1.99	-5.04	0.51
Model D	-0.17	-1.04	-1.85	-5.10	0.49
Model E	-0.24	-1.15	-1.98	-5.03	0.50

Table S11. Computed nitrogen hyperfine and nuclear quadrupole tensors for N_5 in the different models for Cu^{II}SODm in a DMSO:toluene solution. ($\mathbf{A_z}$ is perpendicular to the plane of **L**, $\mathbf{A_y}$ is pointing in the direction of the copper ion. The largest nuclear quadrupole coupling is approximately along $\mathbf{A_x}$, the smallest nuclear quadrupole value (in absolute value) is lying approximately perpendicular to the **L** plane).

	A_x/MHz	A_y/MHz	A_z/MHz	e^2qQ/h /MHz	η
Model A	38.23	48.01	39.85	3.676	0.317
Model B	35.76	45.30	37.31	3.705	0.313
Model C	33.25	42.16	34.74	3.725	0.480
Model D	32.85	41.48	34.37	3.775	0.540
Model E	35.19	44.33	36.76	3.696	0.469

Table S12. Computed nitrogen hyperfine and nuclear quadrupole tensors for N_4 in the different models for Cu^{II}SODm in a DMSO:toluene solution. ($\mathbf{A_z}$ and $\mathbf{P_z}$ are perpendicular to the plane of **L**, $\mathbf{P_x}$ is approximately parallel to $\mathbf{A_y}$).

	A_x/MHz	A_y/MHz	A_z/MHz	e^2qQ/h /MHz	η
Model A	1.00	0.05	0.29	-5.01	0.66
Model B	1.96	0.95	1.17	-5.13	0.63
Model C	1.60	0.67	0.88	-5.02	0.62
Model D	1.56	0.67	0.87	-4.94	0.60
Model E	0.90	0.02	0.25	-4.90	0.66

Table S13. Computed nitrogen hyperfine and nuclear quadrupole tensors for N_3 in the different models for Cu^{II}SODm in a DMSO:toluene solution. ($\mathbf{A_z}$ is perpendicular to the plane of **L,** $\mathbf{P_z}$ lies along $\mathbf{A_y}$, $\mathbf{P_y}$ is approximately perpendicular to **L)**

	A_x/MHz	A_y/MHz	A_z/MHz	e^2qQ/h /MHz	η
Model A	0.10	-0.08	-0.12	-3.40	0.27
Model B	0.14	-0.03	-0.07	-3.41	0.28
Model C	0.13	-0.09	-0.05	-3.41	0.27
Model D	0.12	-0.06	-0.10	-3.41	0.27
Model E	0.09	-0.09	-0.12	-3.39	0.26

Comparison of SOD activities of different SOD mimics

Table S14. SOD activity of various SODm (including Cu^{II}SODm), together with the activity of native SOD from different sources.

Ligand class	IC_{50} (μM)	Reference
Cu^{II}SODm	0.38	Present study
Sulfonamide deriv.	0.1 - 0.3	7
Benzimidazole deriv.	0.1 - 0.34	8
Aminoacids	0.1 – 0.3	9
Pyridazine deriv.	0.4 – 1.63	10
Thiosemicarbozene deriv.	4.0 – 6.7	11
Cyclodextrin deriv.	0.57 – 0.78	12
Phenantroline, bypyridil deriv.	12.0 – 22.0	13
Aspirinate deriv.	1.23 – 1.80	14
Quinoxaline	18.0 – 89.0	15
SOD - horseradish	0.07	70
SOD - bovine	0.04	71
Polypyridilamine deriv.	0.54 – 12.50	72